Scientific Research Publishing

Open Journal of Composite Materials, 2017, 7, 207-217
http://www.scirp.org/journal/ojcm
ISSN Online: 2164-5655
ISSN Print: 2164-5612

Improvement of Bending Strength of Carbon Fiber/Thermoplastic Epoxy Composites

—Effects of Molecular Weight of Epoxy on Carbon Fiber/Matrix Interfacial Strength and Connection of Cracks in Matrix

Hironori Nishida[1,3], Kazuya Okubo[2], Toru Fujii[2], Valter Carvelli[4]

[1]Graduate School of Doshisha University, Tatara Kyotanabe, Kyoto, Japan
[2]Department of Mechanical Engineering and Systems, Doshisha University, Tatara Kyotanabe, Kyoto, Japan
[3]Western Region Industrial Research Center, Hiroshima Prefectural Technology Research Institute, Kure, Hiroshima, Japan
[4]Department of A.B.C., Politecnico di Milano, Milan, Italy
Email: eup1504@mail4.doshisha.ac.jp

How to cite this paper: Nishida, H., Okubo, K., Fujii, T. and Carvelli, V. (2017) Improvement of Bending Strength of Carbon Fiber/Thermoplastic Epoxy Composites. *Open Journal of Composite Materials*, **7**, 207-217.
https://doi.org/10.4236/ojcm.2017.74014

Received: June 1, 2017
Accepted: July 24, 2017
Published: July 27, 2017

Abstract

The bending strength of carbon fiber/thermoplastic epoxy composites (CF/TP-EP Compo.) had bi-linear increase with increase of weight-average molecular weight (Mw) of matrix. The transition in the bending strength appeared at around 55k of Mw ("k" means 10^3). SEM observation of fractured surface of CF/TP-EP Compo. showed that the fracture mode changed from interfacial failure to fiber breakage dominated failure. The smooth surface of carbon fibers appeared at lower Mw than 55k while some resin remained on the fibers indicating good adhesion between carbon fiber and matrix at higher Mw than 55k. The interfacial shear strength between carbon fiber and matrix bi-linearly increased with an increase of Mw similarly to the bending strength of the composite, measured by the micro droplet test. The dynamic loss tanδ of the matrix measured at 2 Hz also showed a bi-linear relationship with respect to Mw having a knee point at Mw = 55k. The connection probability of two cracks introduced on each side of specimens also confirmed that the interfacial strength between carbon fiber and matrix is the key for the mechanical performance of CF/TP-EP Compo. in bending.

Keywords

Thermoplastic Epoxy Composites, Weight-Average Molecular Weight, Interfacial Shear Strength, Crack Propagation, Crack Connecting Probability

1. Introduction

Recent developments in carbon fiber reinforced thermoplastics (CFRTP) have

attracted more interest of aerospace, automotive industries [1] [2] [3] [4] [5] [6] [7]. Due to the use of thermoplastics (TP), CFRTP has superior advantages such as higher toughness, better recyclability and shorter production time than thermoset plastics based composites. Much effort was made to bring the full potential of CFRTP out as well as to reduce their cost. However, the viscosity of conventional thermoplastics even at higher melting temperature is much higher than that of thermoset plastics such as epoxy and vinyl ester. Such high viscosity of TP makes the resin infusion process difficult, resulting poor impregnation of the resin into carbon fibers. Therefore, various impregnation methods have been studied. A method was proposed for reducing the viscosity of TP with a solvent [8]. However, the solvent must be removed during fabricating the composite. Spraying TP powders as well as commingled yarns with TP fibers were also developed to solve the poor resin impregnation into carbon fibers [9] [10] [11] [12] [13]. Fine TP powders were sprayed on to carbon fibers [10] [11], but the powders can be easily removed from the fibers.

Recently, CFRTP using in-situ resin have gotten a lot of attention [14] [15], in which thermoplastic epoxy (TP-EP) was used. TP-EP is without crosslinked structure. Weight-average molecular weight (Mw) of TP-EP depends on the polymerization temperature and the polymerization time [16]. The mechanical properties of TP-EP strongly depend on Mw [17] [18]. (Mw takes into account the molecular weight of a chain in determining the average molecular weight. When the chain is massive, the chain contribution to Mw increases. Mw is often used in the evaluation of the physical properties of the resin.) The bending strength of carbon fiber/thermoplastic epoxy composites (CF/TP-EP Compo.) increased with an increase of Mw as shown in **Figure 1**. The transition in the bending strength appeared at around Mw = 55k ("k" means 10^3). In conjunction with Mw change, fractured surfaces of the composite were different. SEM observations of fractured surface of CF/TP-EP Compo. showed that the fracture mode changed from interfacial failure to fiber breakage dominated failure. **Figure 2(a)** and **Figure 2(b)** show the enlarged fractured surfaces of two samples. Smooth surface of carbon fibers appears in the case of lower Mw than 55k while some resin still sticks on the carbon fibers when Mw is higher than 55k [19].

However, no mechanisms have been well understood for the above results

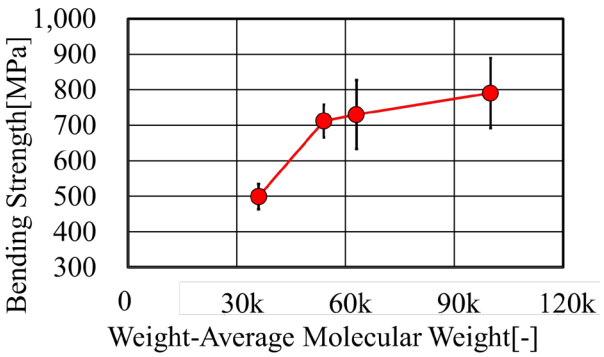

Figure 1. Variations of bending strength with respect to Mw.

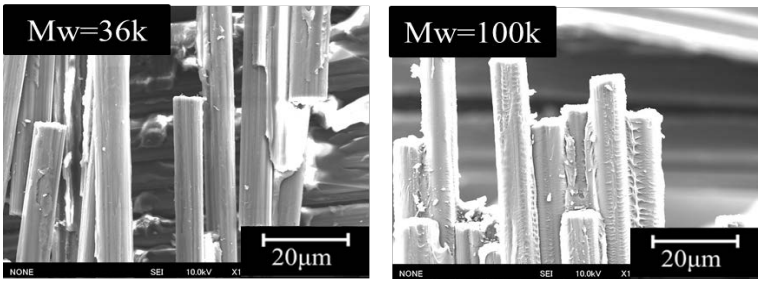

(a) (b)

Figure 2. Fractured surfaces of specimens after three-point bending test. (a) Mw = 36k; (b) Mw = 100k.

(Figure 1). In order to establish the right mechanism, additional mechanical tests are necessary, revealing the effect of Mw on the bending strength of CFRTP using TP-EP. Some relationships such as the one between Mw and interfacial strength of carbon fiber and TP-EP must be helpful for considering the above goal. The investigation also focuses on the crack propagation in fiber yarns embedded specimens for different Mw of matrix.

2. Materials and Experimental Method

2.1. Materials

Plain weave carbon fiber fabric (Mitsubishi Rayon TR3110MS) was used as reinforcement (yarn TR30S 3L, linear density 1.79 g/cm^3, pick and end counts 12.5 inch, areal weight 200 g/m^2). Thermoplastic epoxy resin (DENATITE XNR 6850A, ACCELERATOR XNH 6850B; supplied by Nagase ChemteX Corporation, Japan) was used as matrix (Glass transition temperature: Tg was approximately 100˚C).

2.2. Micro-Droplet Tests

It is well known that the interfacial strength between reinforcing fiber and polymer matrix is the key for the mechanical performance of composites. Therefore, we conducted micro-droplet tests to directly measure the interfacial shear strength between carbon fiber and TP-EP. Figure 3 shows a scheme of the micro-droplet test setup. Both ends of a single carbon fiber were fixed on a sheet of paper using an epoxy-based adhesive. One micro-droplet of TP-EP was attached to the single carbon fiber by a needle attached on a soldering copper. The fiber was pulled out from the droplet at a speed of 0.12 mm/min. Since the maximum load for each test was widely scattered, twenty samples were tested. Equation (1) was used to estimate the interfacial shear strength (τ):

$$\tau = \frac{F}{\pi DL} \tag{1}$$

τ : interfacial shear strength [MPa];
F : Pullout load [N];
D : Fiber diameter [mm];
L : Embedded length [mm].

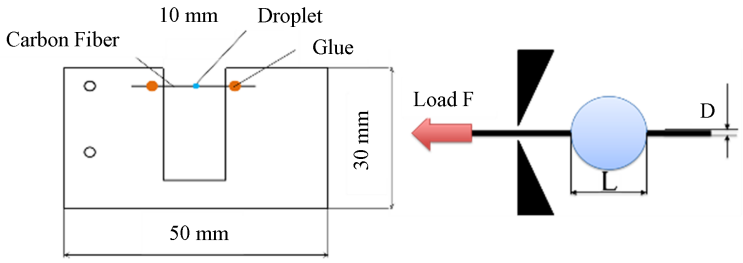

Figure 3. Specimen for micro-droplet test.

2.3. Dynamic Viscoelasticity Tests

Solid TP-EP is generally brittle at low Mw. It becomes tough with an increase of Mw, which indicates that the viscosity measured under cyclic loading could be reflect the level of Mw. Based on this idea, we measured the damping of CF/TP-EP Compo. by the dynamic viscoelasticity test.

First, CF/TP-EP Compo. laminates were made by the following procedure:

1) The resin, "XNR6850A", was heated by using an electric oven at 120˚C;

2) When the temperature of the resin reached 105˚C, the accelerator "XNH6850B" was added to the resin with stirring;

3) The plain weave carbon fabric was impregnated with the TP-EP resin by hand lay-up;

4) CF/TP-EP Compo. prepreg impregnated with the thermoplastic epoxy resin in the state of oligomer was polymerized at a given temperature in an electric oven;

5) The obtained prepreg was cut into 245 × 245 mm and dried at 50˚C for 12 hours;

6) CF/TP-EP Compo. laminates were prepared by press molding with 10 layers of dry prepreg at 175˚C - 195˚C and 6 - 12 MPa on a heat-press device.

Then, the laminate was cut into specimens whose dimensions were shown in Figure 4. Double lap specimens were assembled using parallel sided laminates, aluminum plates, bolts of M6, nuts, washers and aluminum collars as shown in Figure 5. Two strain gages were glued on the aluminum plate and CF/TP-EP Compo. laminate of each specimen to measure the longitudinal strain variation with respect to time under cyclic loading. Here, the specimens were cyclically pulled at 2 Hz of frequency and 0.1 of stress ratio.

Finally, the hysteresis loop of each specimen in the stress-stain relation was plotted to estimate tan (δ) reflecting the degree of viscosity of the laminate. The tangent of loss angle designated as tan (δ) was calculated by the following Equation (2) [20]:

$$\tan\delta = \frac{U_H}{\pi\sigma_0\varepsilon_0} \tag{2}$$

U_H: Hysteresis loss [MPa] = Loop area;

σ_0: Mean stress amplitude [MPa];

ε_0: Mean strain amplitude [−].

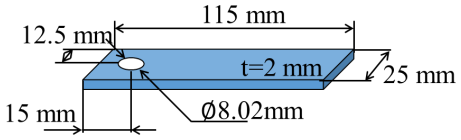

Figure 4. Geometry of CFRTP specimen.

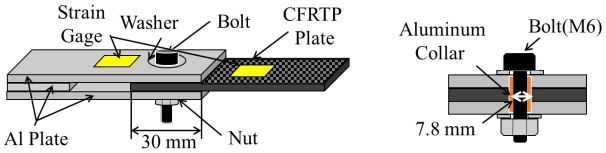

Figure 5. Geometry of specimen for measurement of tan(δ).

2.4. Matrix Crack Tests around the Carbon Fiber

In order to identify the difference in the matrix behavior around a single fiber due to Mw, tensile tests were conducted for TP-EP where a single fiber had been embedded in the longitudinal direction parallel to the loading direction. Single carbon fiber embedded specimens were made by the following procedure. First, a single carbon fiber was extracted from the carbon fiber cloth as explained in Section 2.1. Next, the single carbon fiber was placed on a release agent treated aluminum plate while a slight tension load was applied to the fiber. Then, TP-EP resin was poured onto the plate where the single fiber was set. The plate was kept in an electric oven for a predetermined time and temperature to get the specified Mw. After polymerization, TP-EP plate where a single carbon fiber had been embedded was removed from the aluminum plate. The TP-EP plate was cut into specimens shown in **Figure 6**. By observing with a polarizing microscope in the specimen under loading, the change in stress state around the carbon fiber was visualized.

2.5. Crack Path Observation across Fiber Yarn from a Notch or Two-Sided Notches

Transverse matrix cracks/fiber deboning perpendicular to the loading direction generally initiate in the weakest layer prior to the final failure. As the applied tensile load increases they grow along the fiber yarn(s) at an early stage of loading without cutting the yarn(s) if the interfacial strength between fiber and polymer matrix is weak. On the other hand, they are arrested and created an obstacle to the crack propagation if the interfacial strength is strong. Then, they straightly grow and cross the fiber yarn(s), cutting the yarn(s), resulting in the final failure of the composite. In this test, we expect to reveal how Mw affects the crack growth across the carbon fiber yarn. Two types of test specimens shown in **Figure 7** were prepared. The fabrication process of the specimens is almost the same as Section 2.4. Instead of a single carbon fiber, a 3K fiber yarn was used. Specimen for test A had a pre-crack introduced by the razor blade at the tip of the notch while specimen for test B had two pre-cracks alternately introduced by the razor blade at the notches tip. The offset distances (a) between two notches were altered 0, 1 and 3 mm. The Digital Image Correlation (DIC) method was used to know the strain distribution on

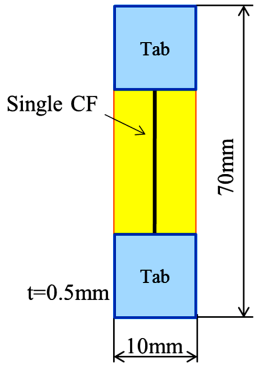

Figure 6. Geometry of single carbon fiber embedded specimens.

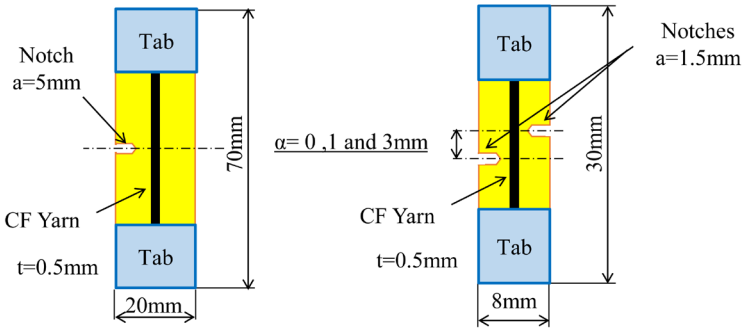

Figure 7. Geometry of a carbon fiber yarn embedded specimens. (a) One notch specimen for Test A; (b) Two sided notches specimen for Test B.

the specimens. The connection probability of two cracks was defined as the probability the two side cracks connect each other during loading.

3. Results and Discussion

3.1. Interfacial Strength of Carbon Fiber/Matrix

Figure 8 shows the relationship between Mw and interfacial shear strength estimated from the micro-droplet test. The relationship can be represented by a bi-linear curve where the transition Mw is about 55k. The interfacial strength does not increase with an increase of Mw beyond this point. A good correlation exists between two relationships, interfacial shear strength vs. Mw and bending strength vs. Mw. As well known that, bending strength decrease if the interfacial strength decreases due to less stress re-distribution ability. The variation of bending strength of CF/TP-EP Compo. with respect to Mw is due to the interfacial strength variation with respect to Mw. Highly polymerization of the matrix is effective to increase the interfacial shear strength between the carbon fiber and TP-EP although it has not been clear why the interfacial strength increases with an increase of Mw. Figure 9 shows the SEM photographs of fractured surface of micro-droplets after the micro-droplet test. Smooth surface of carbon fiber was observed with resin of Mw = 25k (Figure 9(a)), while considering Mw = 90k, better adhesion is confirmed by some residual matrix still bounded to the fiber (Figure 9(b)).

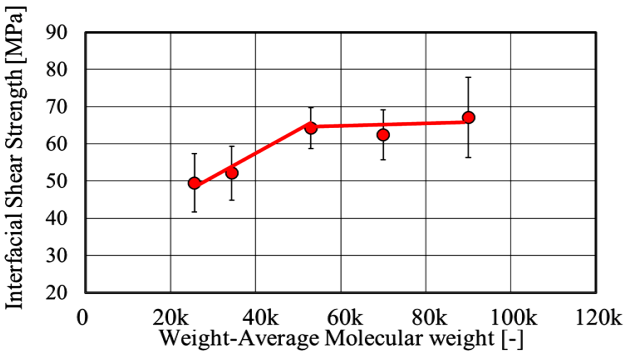

Figure 8. Micro-droplet test: interfacial shear strength vs. Mw.

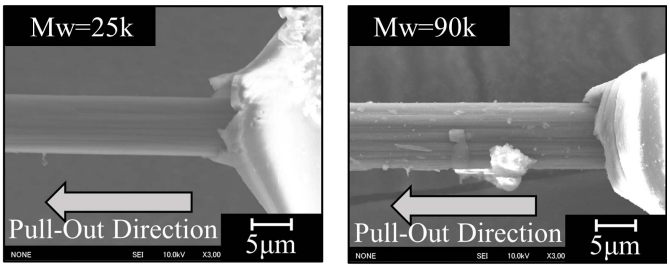

(a) (b)

Figure 9. Carbon fiber surfaces after micro-droplet test. (a) Mw = 25k; (b) Mw = 90k.

3.2. The Tangent of the Loss Angle tan(δ)

Figure 10 shows a hysteresis loop obtained by the dynamic viscoelasticity test. The hysteresis losses for Mw = 46k, 80k and 122k were 0.24, 0.56 and 1.46 [kPa], respectively. Figure 11 shows relationship between Mw and tan(δ) of the matrix calculated on the basis of this hysteresis loss. Tan(δ) of the matrix was improved due to increase of the Mw of the matrix. The correlation between adhesion of polymer material and tan(δ) had been reported in previous study [20]. This shows the enhancement of the adhesion between carbon fiber and matrix in CFRTP, as in the present investigation.

3.3. Crack Initiation of Matrix around Carbon Fiber

Figure 12 shows, for Mw = 43k, cracks in the matrix when 0.25% extension strain was imparted to the test piece, and thereafter the failure immediately after extension strain reached 1.50%. When the Mw of the matrix was Mw = 89k, cracks of the matrix occurred at 1.50% extension strain ;thereafter when extension strain was 2.00% the fiber break occurred and for a strain level of 4.60%, the specimen failed. From this, it was considered that occurrence of initial cracks in the matrix around the carbon fibers was delayed when the Mw of the matrix was high.

3.4. Observing Path of Crack Propagation

Figure 13 shows the maximum principle strain distribution for specimens with

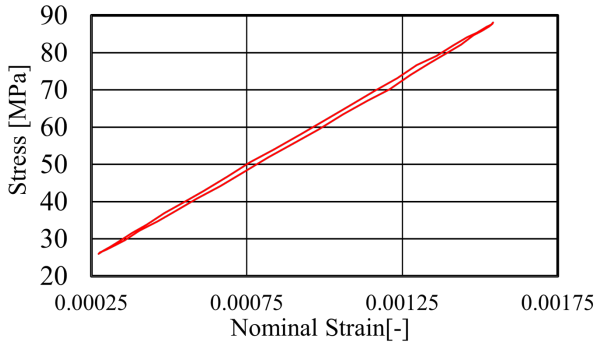

Figure 10. Hysteresis loop (Mw = 122k).

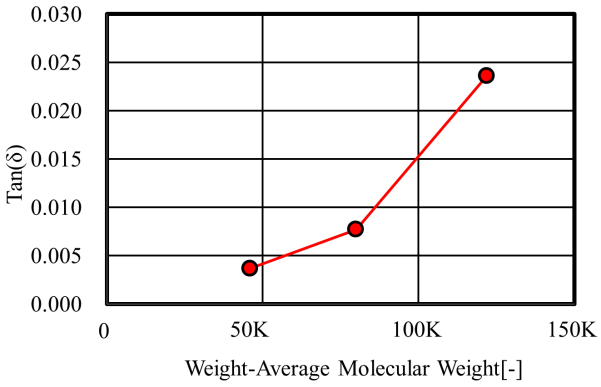

Figure 11. Relationship between tangent of loss angle (tanδ) and Mw.

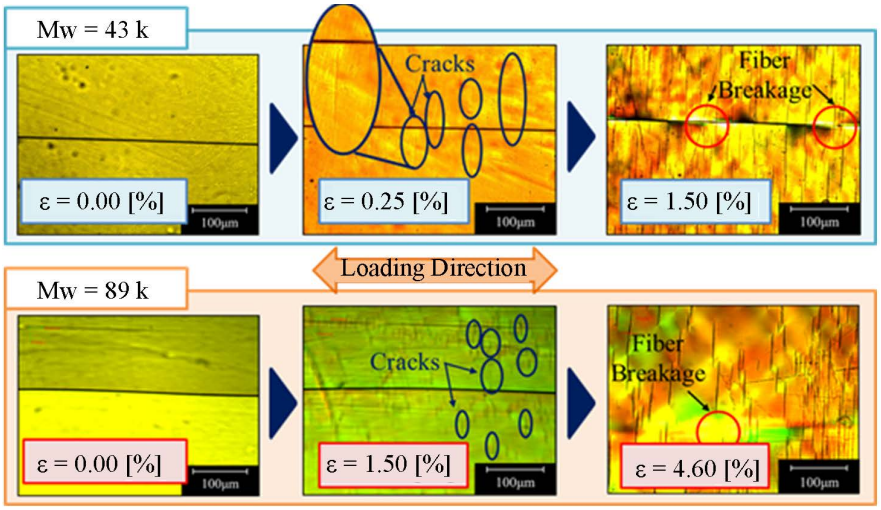

Figure 12. States of matrix cracks around carbon fiber.

Mw were 35k and 73k, respectively. In the case of Mw = 35k , matrix with low Mw, the crack reached the surface of the carbon fiber yarn with remarkable strain concentration when the applied nominal tensile stress reached about 3 MPa. After that, when the stress reached about 11 MPa, the macro crack propagated along the carbon fiber yarn and the fracture immediately occurred. On the other hand, in the case of high Mw (73k),

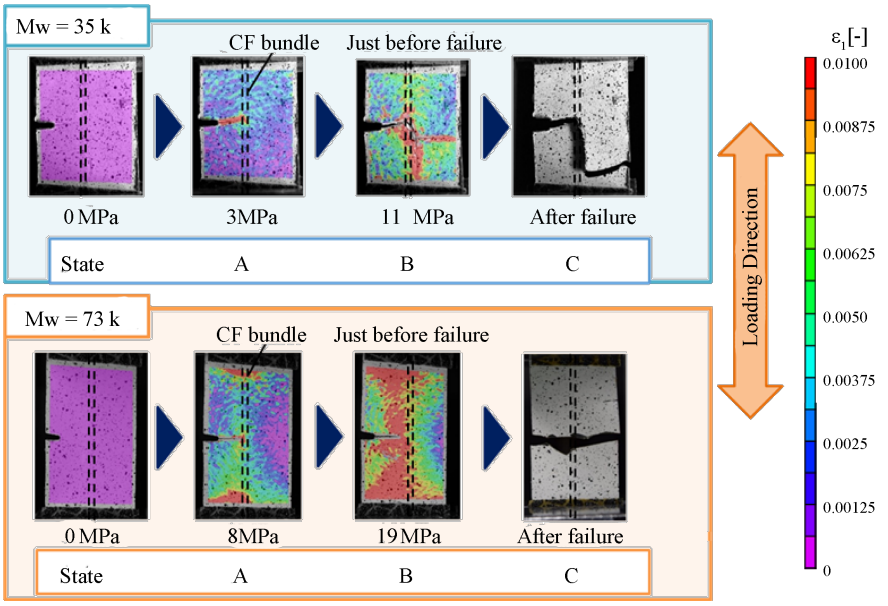

Figure 13. Paths of matrix crack propagation around carbon fiber yarn. A: Condition where crack reached the carbon fiber surface; B: Condition just before breaking of specimen; C: Status of specimen after fracture.

cracks do not progress even when the tensile stress reaches about 3 MPa. When the stress was about 8MPa, cracks reached the surface of the carbon fiber yarn. From those observations, it was found that the cracks interfacial propagating along the fiber yarn prevented as the Mw of the matrix was increased.

3.5. Investigation of Probability of Matrix Crack Connection

Figure 14 shows the relationship between the probability of matrix crack connection and offset distance of the carbon fiber embedded specimen with notches on both sides. In the case that the notches offset distance (α) was 0 mm, matrix cracks connection was not significantly affected by the Mw of the matrix. On the other hand, in the case of the offset distance (α) were 1 mm and 3 mm, the connection probability of the cracks was decreased with increasing Mw of the matrix. This is related to the improvement of the interfacial shear strength with the increase in the molecular weight of the matrix leading to the modification of the crack path. Therefore, we can suppose that the increase of bending strength of CFRTP observed in **Figure 1** is due to the delay of the connection of micro cracks in the matrix when high-polymerization of the matrix was successively achieved.

4. Conclusions

-The crack propagation path changed by improving the interfacial shear strength due to an increase in the Mw of matrix.

-The occurrence of cracks in the matrix around carbon fibers were delayed by an increase in Mw of matrix.

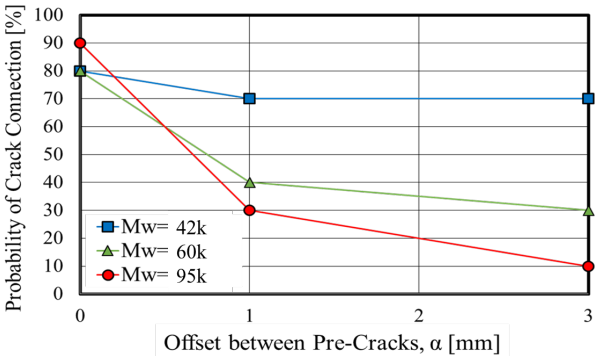

Figure 14. Comparisons of probabilities of crack connections.

-The bending strength of CFRTP was improved due to the delay of the connection of micro cracks in the matrix when high-polymerization of the matrix was successively achieved.

Acknowledgements

The authors are grateful for support of Doshisha University Research & Development Center for Advanced Composite Materials and Nagase Chemtex Corporation, Japan.

We thank helpful contributions in the experiments by Mr. Keisuke Nagai and Mr. Souichirou Imagawa who were graduate students of Doshisha University.

References

[1] Erber, A. and Spitko, S. (2014) Expanded Role for Thermoplastic Composites, *Reinforced Plastics*, **58**, 29-33.

[2] Brady, P. and Brady, M. (2007) Automotive Composites: Which Way Are We Going? *Reinforced Plastics*, **51**, 32-35.

[3] Brady, M. and Brady, P. (2007) Automotive Composites—the Search for Efficiency, Value and Performance. *Reinforced Plastics*, **51**, 26-29.

[4] Stewart, R. (2010) Automotive Composites Offer Lighter Solutions. *Reinforced Plastics*, **54**, 22-28.

[5] Marsh, G. (2013) Composites Poised to Transform Airline Economics. *Reinforced Plastics*, **57**, 18-24.

[6] Klimke, J. and Rothmann, D. (2010) Carbon Composite Materials in Modern Yacht Building. *Reinforced Plastics*, **54**, 24-27.

[7] Brady, M. and Brady, P. (2010) Technology Developments in Automotive Composites. *Reinforced Plastics*, **54**, 25-29.

[8] Liu, B., Xu, A. and Bao, L. (2015) Preparation of Carbon Fiber-Reinforced Thermoplastics with High Fiber Volume Fraction and High Heat-Resistant Properties. *Journal of Thermoplastic Composite Materials*, **30**, 724-737. https://doi.org/10.1177/0892705715610408

[9] Xu, A., Bao, L., Nishida, M. and Yamanaka, A. (2013) Molding of PBO Fabric Reinforced Thermoplastic Composite to Achieve High Fiber Volume Fraction. *Polymer Composites*, **34**, 953-958. https://doi.org/10.1002/pc.22501

[10] Chen, J.H., Schulz, E., Bohse, J. and Hinrichsen, G. (1999) Effect of Fiber Content

on the Interlaminar Fracture Toughness of Unidirectional Glass/Fiber Polyamide Composite. *Composites: Part A*, **30**, 747-755.

[11] Mohanty, A.K., Drzal, L.T. and Misra, M. (2002) Engineered Natural Fiber Reinforced Polypropylene Composites Influence of Surface Modifications and Novel Powder Impregnation Processing. *Journal of Adhesion Science and Technology*, **16**, 999-1015. https://doi.org/10.1163/156856102760146129

[12] Long, A.C., Wilks, C.E. and Rudd, C.D. (2001) Experimental Characterization of the Consolidation of a Commingled Glass/Polypropylene Composite. *Composites Science and Technology*, **61**, 1591-1603. https://doi.org/10.1016/S0266-3538(01)00059-8

[13] Ye, L., Friedrich, K., Kästel, J. and Mai, Y. (1995) Consolidation of Unidirectional CF/PEEK Composites from Commingled Yarn Prepreg. *Composites Science and Technology*, **54**, 349-358. https://doi.org/10.1016/0266-3538(95)00061-5

[14] Ben, G. and Sakata, K. (2015) Fast Fabrication Method and Evaluation of Performance of Hybrid FRTPs for Applying Them to Automotive Structural Members. *Composite Structures*, **133**, 1160-1167. https://doi.org/10.1016/j.compstruct.2015.07.093

[15] Hirabayashi, A., Ben, G. and Ozeki, H. (2013) Heat Resistance Properties of FRTP Composed of In-Situ Polymerization PA6 and CF and GF Fabrics. *Proceedings of* 19*th International Conference on Composite Materials*, Montreal, 23 July-2 August 2013, 1581-1588.

[16] Nishida, H. (2015) The Development of Thermoplastic Epoxy Resin and Continuous Fiber Reinforced Thermoplastics Using it. *Journal of the Adhesion Society of Japan*, **51**, 516-523.

[17] Imanishi, T., Nishida, H., Hirayama, N. and Tomomitsu, N. (2007) In Situ Polymerizable Thermoplastic Epoxy Resin and High Performance FRTP Using It and Fiber Fabrics. *Proceedings of* 16*th International Conference on Composite Materials*, Kyoto, 8-13 July 2007, 194-195.

[18] Nishida, H. (2011) Aiming to Create Novel Composites. *Journal of the Adhesion Society of Japan*, **47**, 361-368. https://doi.org/10.11618/adhesion.47.361

[19] Nagai, K., Nishida, H., Okubo, K. and Fujii, T. (2016) Static and Fatigue Bending Properties of CFRTP with Highly Polymerized Thermo-Plastic Epoxy for Matrix. *Proceedings of the* 10*th Asian-Australasian Conference on Composite Materials*, Busan, 16-19 October 2016, File.T15-3.

[20] Jensen, M.K., Bach, A., Hassager, O. and Skov, A.L. (2009) Linear Rheology of Cross Linked Polypropylene Oxide as a Pressure Sensitive Adhesive. *International Journal of Adhesion & Adhesives*, **29**, 687-669. https://doi.org/10.1016/j.ijadhadh.2008.10.005